Lambda Dynamics in GROMOS05 Using Newtonian Equations of Motion

Using B&S-LEUS for Enhanced Sampling

BSc Thesis

by

Rico Häuselmann ricoh@student.ethz.ch

Supervised by

Noah Bieler Supervisor
Philippe H. Hünenberger Supervising Professor

July 25, 2012

Lambda dynamics (LD), a recent method[?] for free energy calculations was implemented in the GROMOS05[?] package for molecular dynamics (MD) simulations. The LD method, contrary to other methods such as free energy perturbation (FEP) and thermodynamic integration (TI), treats the coupling parameter between states (λ) as an additional degree of freedom following Newtonian dynamics.

After implementing the method into GROMOS05, it was connected with Ball-and-Stick local elevation umbrella sampling (B&S-LEUS)[?], recently implemented in GROMOS05, simulations were run on a test system (section 2.2) in order to explore parameter sensitivity and to find a working B&S-LEUS procedure. Due to a limited amount of time no complete working case can be presented though the results obtained were quite promising (Figure 3.10).

A TI was run of the test system as a reference, yielding a $\Delta\Delta G_{A,B}$ of 211.5 ± 0.6 (subsection 2.1.1). The TI curve for $\Delta G(\lambda)$ is of the same shape as $-U_{bias}$ in four build up runs.

1 Introduction

free energy calculations have been used to investigate many important problems from cavity formations in water[?] to protein[?] and amino acid[?] folding. The relative free energy is a powerful tool for determining all the thermodynamic properties of a system. In 1996[?] a new approach has been investigated, using a dynamic coupling variable λ between states, thus termed LD[?]. It has been suggested by **?**] that this approach, especially when combined with umbrella sampling (US) might provide benefits over the other, more established methods.

US uses a biasing potential U_{bias} to enhance sampling of the conformational space. Often this U_{bias} is provided by local elevation (LE), a technique to build up such a potential by increasing the value of U_{bias} locally at conformations with low potential energy. This combination is often abbreviated as LEUS.

B&S-LEUS is a LEUS scheme giving fine grained control about the subspace to be sampled. The system is constrained to the relevant subspace by choosing a priori circular regions of interest (balls) and combining them with pathways (sticks).

For one thing, the method yields dynamic information about the behaviour of λ. In addition to that, partitioning λ into different contributions for different kinds of interaction and performing LD might lead to additional insight into the choice of reaction paths.

GROMOS[? ?] is an MD package introduced in 1996. It has been continuously updated since then. The lates release is GROMOS05[?], in which the B&S-LEUS[?] US scheme is implemented.

The purpose of this work was to implement basic LD functionality in GROMOS05 and to carry out simulations combining it with B&S-LEUS and if possible to find a working procedure for the determination of the relative free energy difference between two compounds in a test system as a proof-of-concept.

2 Methods

2.1 Free Energy Calculations

In order to calculate the free energy difference ΔG between two different states A and B the system Hamiltonian is partitioned into two Hamiltonians H_A and H_B with λ as a coupling parameter

$$H_{Sys} = (1-\lambda)H_A + \lambda H_B,$$

where $\lambda \in [0,1]$.

2.1.1 Thermodynamic Integration (TI)

In TI the system is simulated at a set of fixed λ points[?]. The relative free energy difference is then calculated according to

$$\Delta\Delta G = \int_0^1 \left\langle \frac{\mathrm{d}H}{\mathrm{d}\Lambda} \right\rangle_\lambda \mathrm{d}\lambda.$$

2.1.2 Lambda Dynamics (LD)

The lambda dynamics approach to free energy calculations was first reported in[?]. This method applies the Newtonian equations of motion to the λ degree of freedom.

$$\ddot{\lambda} = \frac{\mathrm{d}H}{\mathrm{d}\Lambda}\frac{1}{M_\lambda}$$

In this work the dynamics were performed on an internal variable called $\tilde{\lambda}$ which wasn't restrained to $[0,1]$. $\tilde{\lambda}$ was then remapped to the coupling parameter λ using a periodic mapping which mirrors $\tilde{\lambda}$ at the boundaries 0 and 1.

$$\lambda(\tilde{\lambda}) = \begin{cases} 2 - \left|\tilde{\lambda} - 2\left\lfloor\frac{\tilde{\lambda}}{2}\right\rfloor\right|, \text{ if } \left|\tilde{\lambda} - 2\left\lfloor\frac{\tilde{\lambda}}{2}\right\rfloor\right| > 1, \\ \left|\tilde{\lambda} - 2\left\lfloor\frac{\tilde{\lambda}}{2}\right\rfloor\right| \text{ else} \end{cases}$$

The following leap-frog integration scheme was used to implement said equations of motion.

$$v_{\tilde{\lambda}}(t) = v_{\tilde{\lambda}}(t-1) + \Delta t \frac{F_{\tilde{\lambda}}(t)}{m_{\tilde{\lambda}}}$$

$$\tilde{\lambda}(t) = \tilde{\lambda}(t-1) + \Delta t v_{\tilde{\lambda}}(t)$$

2.1.3 Ball & Stick Local Elevation Umbrella Sampling (B&S-LEUS)

US is a technique in MD, where sampling is enhanced by overcoming energy barriers using a bias potential

$$V_{Tot} = V_{Sys} + U_{bias},$$

where the biasing potential counteracts the system's potential to produce a flatter V_{Tot}. After sampling the biased system the free energy difference can be obtained by using $U_{bias}(\lambda)$ as a weighting factor.

$$\Delta G(\lambda) = -k_B T \log p(\lambda) - U_{bias}(\lambda)$$

Such a bias potential can be obtained by LE. In this case a simulation is performed, during which the bias potential is built up to the point, where a mostly flat total potential has been reached. The bias potential from the build up phase is then used in the US phase.

In this work B&S-LEUS[?] is used to perform LEUS of a subspace of $\tilde{\lambda}$. In the B&S-LEUS scheme sampling is confined to a conformational subspace by means of defining "balls" and "sticks" - spherosymetrial and cylindro-symmetriacl, respectively - regions of the conformation space. This results in a set of one dimensional potentials (radial for balls and longitudinal for sticks) discretized into Γ grid points, each with a local function assigned to it.

During the build up procedure the system is simulated and at each step the grid point nearest to the current conformation is increased by an increment k_{LE}. This increment in turn is reduced by a factor f_{red}, each time the whole region has been visited.

The confining of the system to the subspace is realized by placing a half-harmonic potential outside the ends of the region. The height of these wall potentials is determined by the parameter c_{LE}

For the purpose of this work only one single stick is used to keep $\tilde{\lambda}$ in bounds and build up the biasing potential.

2.2 System

A test system (Figure 2.1 was setup in a modified version of GROMOS05[?] using the 53A6 force field[?]. The system contains one molecule of solute in a box of 999 water molecules and simulations were NVT at $T = 298\,K$. 1,4-diphenol was chosen for state A ($\lambda_A = 0$) and benzene for state B ($\lambda_B = 1$). Soft core interactions with $\alpha = 0.5$ were used for the perturbed atoms.

Figure 2.1: The test system. State A, 1,4-diphenol corresponds to $\lambda = 0$, state B, benzene corresponds to $\lambda = 1$.

2.3 Parameters

2.3.1 LD Parameters

In order to explore the behaviour of the system for different LD parameters simulations of the system were run without using B&S-LEUS. First, in subsection 3.1.1 two values for M_λ (10^5 u nm^2 and 10^6 u nm^2) were chosen and combined with $\lambda_0 \in \{0, 0.05, 0.2, 0.4, 1.0\}$. The parameters are listed in Table 3.1. Then a wider range of M_λ was explored in subsection 3.1.2. It was found that the M_λ parameter has a great impact on the convergence and the oscillation speed of $\tilde{\lambda}$. However, λ_0, the starting value for λ was found to be of no great consequence.

Further, it was shown that the oscillatory behaviour of $\tilde{\lambda}$ can be approximated by a harmonic oscillator using the relation between the oscillation period $\langle\tau\rangle$ and the lambda mass of a harmonic oscillator.

2.3.2 B&S-LEUS Parameters

To establish a build up procedure that delivers the desired bias potential in the lowest possible amount of time the available parameters were varied against each other. First k_{LE}, f_{red}, Γ and c_{LE} were varied while using $\tilde{\lambda} \in [0, 2]$ as subspace.

It was found that low k_{LE} (0.005 or lower) are necessary to avoid accelerating lambda past the point of sensitivity to the system's potential.

For $f_{red} = 0.9$ was found to be the optimal value, whereas lower values leading to premature freezing of the bias potential and higher values to increased acceleration as well as elevating all subspace simultaneously, producing essentially steep walls and a flat middle region.

A high number of grid points Γ was found to be too costly whilst bearing too little benefits, so that the use of more than 40 grid points is rendered unjustified.

500 was recognized as a minimum value for c_{LE} with lower values not able to keep $\tilde{\lambda}$ within the chosen subspace.

This information was used to guide the selection of parameters for a second series of B&S-LEUS experiments using a stick from $\tilde{\lambda} = -1$ to $\tilde{\lambda} = 1$. In this series even lower build up constants k_{LE} were explored. This second approach was found to produce promising results, which couldn't be followed on in this work due to time restrictions.

2.4 Computational Details

A modified version of the GROMOS05 program md++[?] was used for all simulations. A leap frog scheme was used for the implementation of Newton's equations of motion for $\tilde{\lambda}$. The mapping from subsection 2.1.2 was used to confine the system λ to the interval $[0, 1]$. For the data analysis, the GROMOS++ suite of programs[?] as well as Python 2.7.2[?] and the Python module NumPy[?] were used. The matplotlib[?] Python module was used exclusively for drawing all the plots.

3 Results

3.1 Plain LD

3.1.1 λ Starting Values

For $M_\lambda = 10^5\,\mathrm{u\,nm^2}$ and $M_\lambda = 10^6\,\mathrm{u\,nm^2}$ different starting values (Table 3.1) of λ_0 were chosen and the systems were then simulated for 5 ns in order to explore the impact of λ_0 on the simulation in terms of convergence.

M_λ	$10^5\,\mathrm{u\,nm^2}$					$10^6\,\mathrm{u\,nm^2}$			
λ_0	0	0.05	0.2	0.4	1.0	0	0.05	0.2	0.4

Table 3.1: This table shows the different starting points chosen for the respective lambda masses.

The $\tilde{\lambda}$-trajectories are shown in Figure 3.1. There and even better in Figure 3.2 it can be seen that the choice of starting lambda has moderate impact on the time needed for the system to equilibrate, as opposed to M_λ. Masses considerably higher than $10^6\,\mathrm{u\,nm^2}$ were considered too slow converging for practical purposes.

In order to show the equilibration process even better a plot was drawn depicting only peak points of the $\lambda(t)$ curve, where the oscillations in between are left away. This made it possible to superimpose curves for the various runs for better comparison. This is shown in Figure 3.2.

3.1.2 Lambda Mass

The range of M_λ between 1 and $2^{18}\,\mathrm{u\,nm^2}$ was systematically explored by running 10 simulations with exponentially increasing masses. The increasing oscillation frequency with decreasing mass was taken into account by choosing smaller time steps (dt) with lower masses. As the $\tilde{\lambda}$ behaves somewhat like a harmonic oscillator, $\Delta dt \propto \sqrt{\Delta M_\lambda}$ was chosen. The exact parameters of the 10 runs are summarized in Table 3.2. The main point of interest was how the mass would influence the way $\tilde{\lambda}$ couples to the system. As the oscillation period is influenced by the mass it was expected to see different dynamics when the timescale of oscillation period was similar to that of water movement than in cases where those were completely different.

In Figure 3.3 the $\tilde{\lambda}$ trajectories of the simulations can be seen. As expected, the amount of steps to equilibration first decreases with the mass. However, for very low masses the number of steps increases again. This might be due to coupling to noise or also to a too big time step as the system can only approximately be treated as a harmonic oscillator.

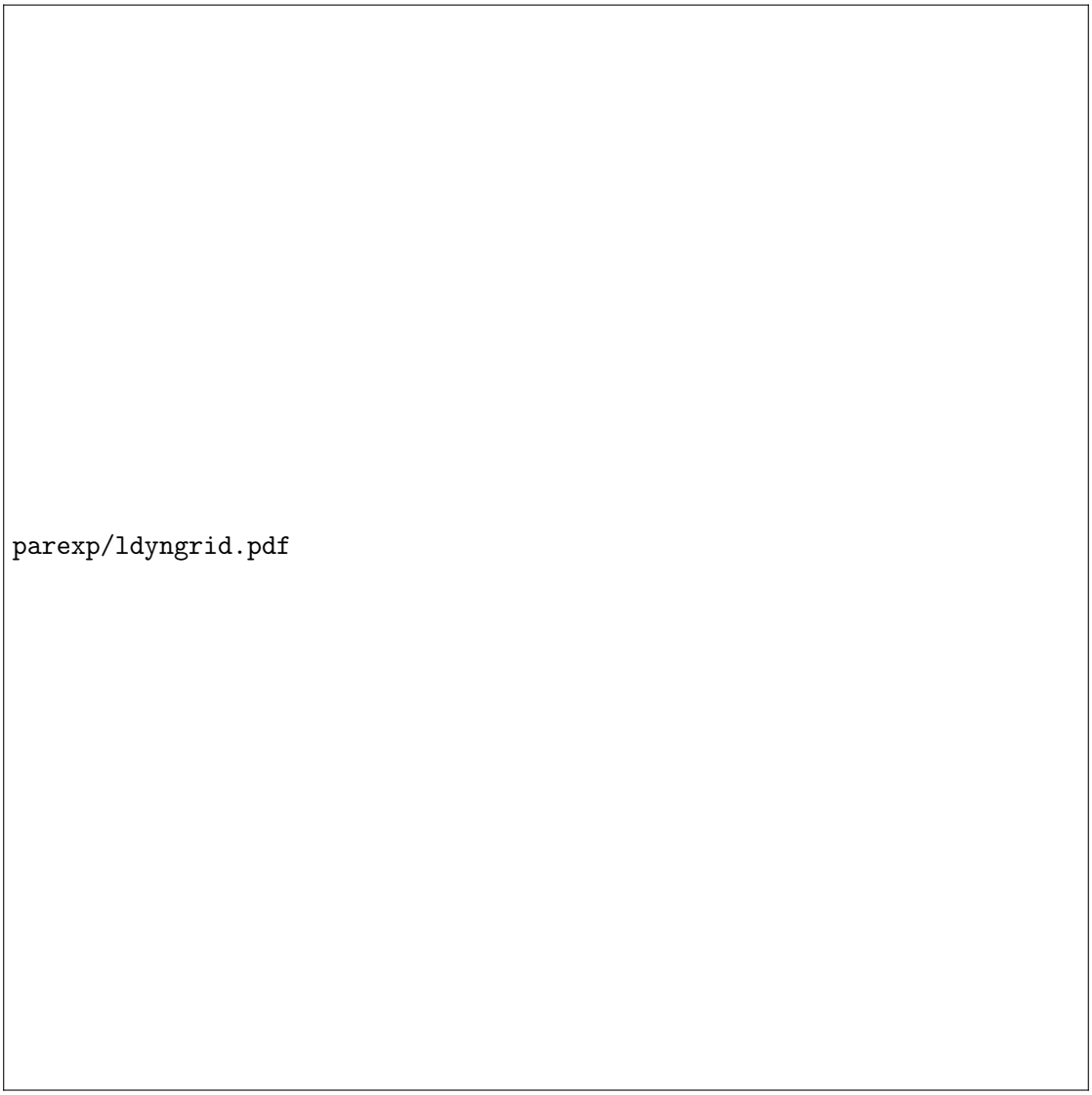

Figure 3.1: Continuous $\tilde{\lambda}$ variable as a function of time. Simulations were run with two different M_λ and different λ_0 for 5 ns. The y scales are chosen according to the value for λ_0. It can be observed that for $M_\lambda = 10^5$ $\tilde{\lambda}$ oscillates and equilibrates faster.

M_λ [u nm^2]	1	2^2	2^4	2^6	2^8	2^{10}	2^{12}	2^{14}	2^{16}	2^{18}
dt [fs]	2	1	2^{-1}	2^{-2}	2^{-3}	2^{-4}	2^{-5}	2^{-6}	2^{-7}	2^{-8}

Table 3.2: The parameters chosen for the simulations exploring impact of M_λ.

In the region of mass with oscillation time scale in the region of water movement (high mass) more variety in amplitudes is observed from peak to peak which might indicate

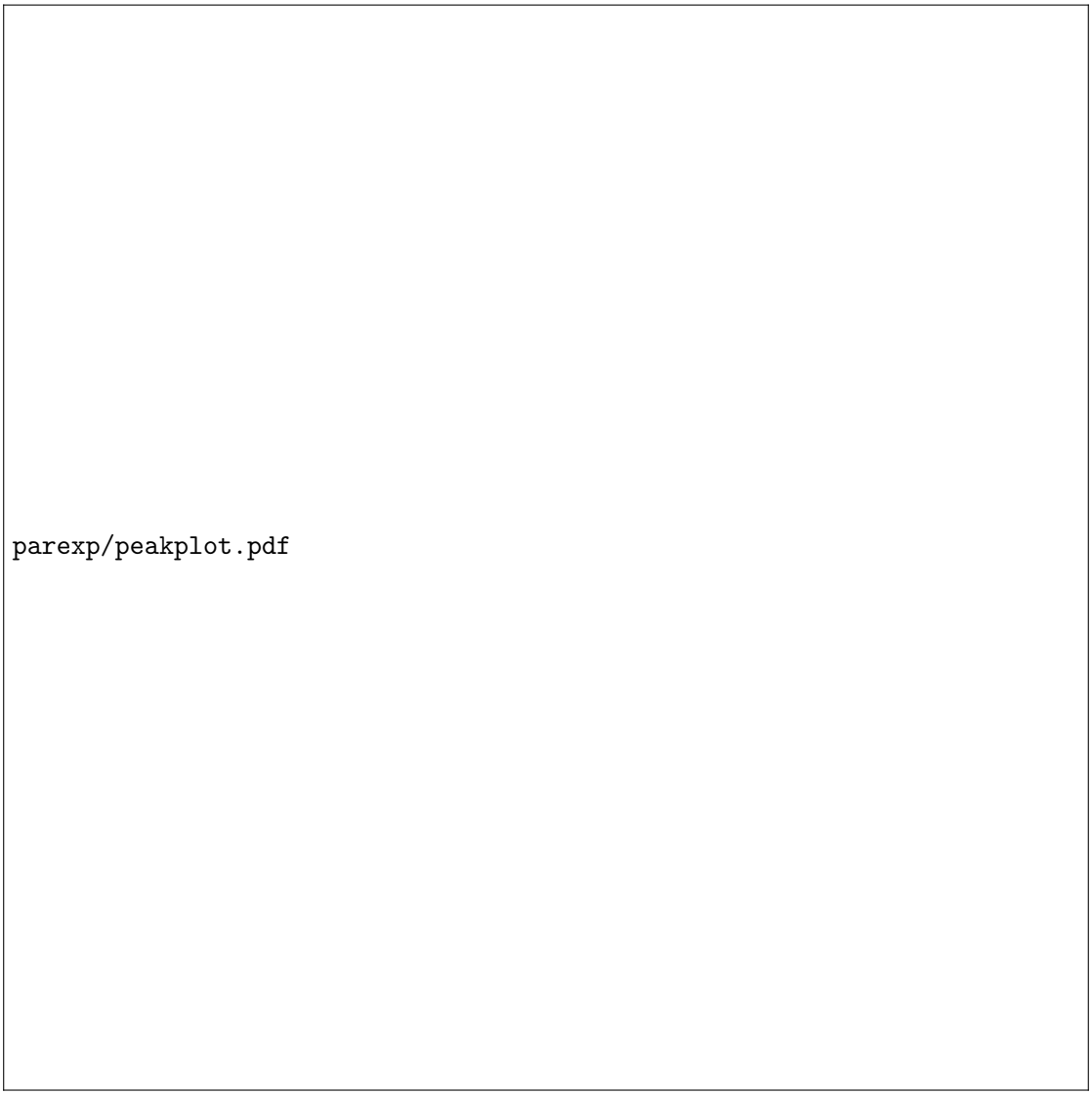

Figure 3.2: The peak positions of the λ variable confined to $[0, 1]$ over time with varying M_λ and λ_0. It can be observed that 2 ns simulation time is enough to equilibrate λ independently of λ_0 for $M_\lambda = 10^5$ but not for $M_\lambda = 10^6$. Also all trajectories seem to converge towards oscillating around zero with an amplitude of about 0.02 (dashed line).

that the $\tilde{\lambda}$ degree of freedom is better coupled to the system.

Figure 3.4 shows a double logarithmic plot of τ over M_λ. The theoretical curve for a harmonic oscillator is drawn as a dashed line. The $\langle\tau\rangle$ was computed by averaging peak to peak distances over the last 1000 time steps. The values for τ_{fft} were obtained by Fourier transforming the last 1000 steps of the $\lambda(t)$ curve and inverting the frequency with the highest contribution.

Figure 3.3: Continuous $\tilde{\lambda}(t)$. The x-axis are scaled according to the different time steps, keeping the length of a simulation step on the x axis constant throughout. In addition to influencing the time needed for convergence there are also effects observed like the higher amplitude of equilibrium oscillations for $M_\lambda = 1\,\mathrm{u\,nm^2}$. Instead of continuously equilibrating faster (in terms of steps) the system takes fewer steps for masses neither too high or low and more steps for very high and very low masses.

Figure 3.4: Double logarithmic plot of the oscillation periods τ of $\lambda(t)$ vs. M_λ. $\langle\tau\rangle$ calculated by averaging, τ_{fft} by a Fourier transform. The dashed line shows the curve for a harmonic oscillator

3.2 TI results

As a reference a TI was run using 31 λ points and an NPT ensemble at $P = 1.019\,\mathrm{MPa}$ with all other parameters (section 2.2) left untouched. The result can be observed in Figure 3.5. The Value obtained for $\Delta\Delta G_{A,B}$ is 211.5 ± 0.6.

Figure 3.5: The $\Delta G(\lambda)$ curve obtained by TI .

3.3 Free Energy Calculations With B&S-LEUS

A wide array of parameter combinations was explored in order to find a suitable build up procedure. At first the stick start and end points were set at 0 and 2 respectively, the subregion of interest was centered around state B (Figures 3.6 to 3.9). As it turned out, it was easier to achieve good results when letting the stick go from -1 to 1, centering it around state A with the potential valley in the middle (Figure 3.10).

The knowledge gained from the first series with B in the center of the stick was used to guide the choice of parameters in the second series.

For further tests even higher values for c_{LE} should be considered.

3.3.1 Biasing Potential Centered Around B

160 simulations were run with all possible combinations of $k_{LE} \in \{0.001, 0.005, 0.01, 0.05, 0.1\}$, $f_{red} \in \{0.7, 0.8, 0.9, 1.0\}$, $\Gamma \in \{20, 40, 60, 80\}$ and $c_{LE} \in \{50, 500\}\,\mathrm{kJ\,mol^{-1}}$. As no complete build up could be produced, only a few examples demonstrating the influence of each parameter shall be shown here. For each of these examples the $\tilde{\lambda}$ trajectories as well as the bias potential are plotted in autoreffig:bsg-kle through Figure 3.9.

In Figure 3.6 the influence of the per-step increment k_{LE} is shown by fixing all other parameters. It is shown that low k_{LE} values are necessary to avoid accelerating $\tilde{\lambda}$ too

much. The acceleration happens when the bias potential is built up at a grid point from which $\tilde{\lambda}$ is moving away. In this case the slope of U_{bias} is increased and so $\tilde{\lambda}$ is accelerated. When $\tilde{\lambda}$ now passes the velocity at which it could be stopped by the system potential barrier it will sweep the entire space indifferently, only slowed down enough at potential barriers of the system to increase the relative build up in that region.

Figure 3.6: Varying k_{LE}. The red dashed line depicts the inverse of the $\Delta G(\lambda)$ resulting from the TI. For values higher than 0.001, the surfing effect lead to velocities high enough to let $\tilde{\lambda}$ sweep easily over the potential barrier located at $\tilde{\lambda} = 1$ easily, only slowing down a bit. This slowing down leads to increased build up in the region of the barrier instead of the potential valley. For $k_{LE} = 0.001$ it is not clear if longer build up time would lead to eventual flattening of the 1-2 region and successive build up of the 0-1 region. The system might be caught between the second to last grid point and the wall potential, note the slight valley at $\tilde{\lambda} = 2$.

Figure 3.7 shows build up runs for different f_{red} values with all other parameters fixed. The red dashed line depicts the inverse of the $\Delta G(\lambda)$ resulting from the TI. It was found that a value of 0.9 delivered the best results. Lower values prevented further build up before the process was completed whilst $f_{red} = 1.0$ (no reduction at all) was shown in combination with surfing to lead to infinite build up of all of the allowed space simultaneously.

Figure 3.7: Different f_{red}. The red dashed line depicts the inverse of the $\Delta G(\lambda)$ resulting from the TI. The choice of f_{red} is important as too high values can cause the system to lose much time in simply sampling the wall potentials as seen in the plot for $f_{red} = 1.0$. Too low however can mean that the system freezes in a disadvantageous state. Note that for $f_{red} = 0.7$ the system wouldn't change much anymore as the per-step increment was already reduced to a very small amount.

A systematic exploration of Γ can be found in Figure 3.8. Raising the number of grid points over 20 was found to have only minor impact on the shape of the bias potential at the cost of precious build up time.

Figure 3.8: Number of grid points Γ. The red dashed line depicts the inverse of the $\Delta G(\lambda)$ resulting from the TI. The higher the number of grid points the less often each grid point is elevated. Thus, higher numbers whilst possibly leading to more accurate bias potentials do so at the price of longer build up times as can be observed here.

Two different values were used for c_{LE}. The higher value used, 500 was found to be the minimum needed to prevent $\tilde{\lambda}$ from breaking out of the influence of the wall potentials

alltogether.

Figure 3.9: Height of the wall potentials c_{LE}. The red dashed line depicts the inverse of the $\Delta G(\lambda)$ resulting from the TI. At the lower value for c_{LE} $\tilde{\lambda}$ can be observed leaving the area it should be confined to and passes the end of the wall potential. With the higher value $\tilde{\lambda}$ is brought back to the confined region when necessary.

3.3.2 Biasing Potential Centered Around A

Using the knowledge from the previous series of experiments with a B centered stick region the parameters for this new series were chosen as shown in Table 3.3. c_{LE} was chosen as $500\,\mathrm{kJ\,mol^{-1}}$ for all the runs.

k_{LE}	f_{red}	Γ	k_{LE}	f_{red}	Γ
0.0001	0.9	20	0.001	0.9	20
0.0001	0.9	40	0.001	0.9	40
0.0001	0.1	20	0.001	0.1	20
0.0001	0.1	40	0.001	0.1	40
0.0005	0.9	20	0.005	0.9	20
0.0005	0.9	40	0.005	0.9	40
0.0005	0.1	20	0.005	0.1	20
0.0005	0.1	40	0.005	0.1	40

Table 3.3: Parameters for the A centered stick simulations.

In Figure 3.10 the results of the simulations with the stick region set around state A are presented. Although the system never leaves the influence region of the stick, for $k_{LE} = 0.005$ and $f_{red} = 0.9$ the systems spends a lot of time in building up the walls. Even if the middle region would be built up correctly, the umbrella sampling might be distorted in these wall regions. For $k_{LE} = 0.005$ and $f_{red} = 1.0$ the familiar problem occurred, where the stick region as a whole is continuously elevated.

The $k_{LE} = 0.001$ runs provide similar results. With $k_{LE} = 0.0005$ $\tilde{\lambda}$ seems to be caught between a wall and the next grid point. This might be alleviated by using higher wall potentials, i.e. c_{LE}.

The results for the lowest $k_{LE} = 0.0001$ however look very promising as can be seen in the four lower right graphs in Figure 3.10. The biasing potential have the right shape and the wall potentials are not built up. On the other hand the build up was clearly not finished after 10 ns. 20 ns runs were started but took too long to get included in this work. The same simulations were also run again with $c_{LE} = 5000$ and 20 ns build up time. These runs, too, couldn't be included here.

Figure 3.10: $\lambda(t)$ and the corresponding biasing potential resulting from the B&S-LEUS buildup procedure. The red dashed line depicts the inverse of the $\Delta G(\lambda)$ resulting from the TI. In most cases the system spent much time building up wall potentials. This indicates that using a higher c_{LE} might yield better results. In some cases the $\tilde{\lambda}$ was caught between the last grid point and the wall potential, further suggesting the use of a greater c_{LE}. Only with the lowest k_{LE} the stick limits were not overstepped, however in those cases the buildup was not complete as not all lambda space has been visited. It was concluded that more time should be given for the buildup process and that increased values for c_{LE} should be tried.

4 Discussion

A suitable build up procedure was found (see subsection 3.3.2 and Figure 3.10). Unfortunately, due to time constraints, the process couldn't be given the amount of time required for a complete build up. Others will further follow this line of work.

The build up stage was found to be sensitive in a greater way than expected to the choice of subspace, obviously running much more efficiently when the maxima of the V_{Sys} coincided with the stick end points. This can be explained by the fact, that then $\tilde{\lambda}$ will naturally tend to oscillate around the middle of the stick region, essentially building up both slopes of the biasing potential at the same time. Conversely, in the case where the minima of the system's potential lie adjacent to the walls, two minima are created both of which must be separately built up. This means that the system will visit and build up the wall regions separately, loosing time in building walls.

The sensitivity to the other parameters was as expected. k_{LE} was found to influence not only the speed of build up but also higher values tend to create large accelerations of the $\tilde{\lambda}$ variable, leading to undesired results (Figure 3.6, Figure 3.10). Too low values for c_{LE} were found to be ineffective in constraining $\tilde{\lambda}$ whilst there are hints as to that higher values might allow choosing higher k_{LE} leading to even faster build ups (Figure 3.9 and Figure 3.10.

Small values for f_{red} (great reduction) were found to prohibit complete building up by reducing the force increment too soon. A value of 1 (no reduction at all) was sometimes found prone to surfing and thus too great acceleration of $\tilde{\lambda}$. See Figure 3.7 and Figure 3.10.

The number of grid points Γ was not shown to have moderate effect on the shape of the biasing potential as well as a strong effect on the time needed for complete build up. Refer to Figure 3.8 for more information.

The parameter range found useful to run the B&S-LEUS build up scheme with was $k_{LE} \approx 10^{-}4$, $c_{LE} >= 500$, $f_{red} = 0.9 - 1.0$, $\Gamma = 20 - 40$.